Hydrogenperoxo-[(bztpen)Fe(OOH)]$^{2+}$ and Its Deprotonation Product Peroxo-[(bztpen)Fe(O_2)]$^{+}$, Studied by EPR and Mössbauer Spectroscopy − Implications for the Electronic Structures of Peroxo Model Complexes

Olivier Horner,*[a] Claudine Jeandey,[a] Jean-Louis Oddou,[a] Pierre Bonville,[b] Christine J. McKenzie,[c] and Jean-Marc Latour[a]

Dedicated to the memory of Prof. William E. Hatfield

Keywords: EPR spectroscopy / Iron / Mössbauer spectroscopy / Peroxo ligands

The purple hydrogenperoxo species [Fe(bztpen)(OOH)]$^{2+}$ (**1**) can be generated in methanol solution by treatment of [Fe(bztpen)Cl]$^{3+}$ with a large excess of hydrogen peroxide [A. Hazell, C. J. McKenzie, L. P. Nielsen, S. Schindler, M. Weitzer, *J. Chem. Soc., Dalton Trans.* **2002**, 310–317]. Addition of 30 equivalents of triethylamine to a solution of [Fe(bztpen)(OOH)]$^{2+}$ gives the [Fe(bztpen)(O_2)]$^{+}$ (**2**) species, in which it has been proposed that the peroxo ligand is coordinated in the η^2 mode. We have synthesized both 100% ^{57}Fe-enriched non-heme Fe^{III} peroxo species and studied them by EPR and Mössbauer spectroscopy. Species **1** displays a typical S = 1/2 low-spin ferric EPR spectrum, the g values of which have been analysed in terms of the Griffith model [J. S. Griffith, *Proc. R. Soc. London, A* **1956**, *234*, 23–36]. We have thus obtained insight into the electronic structure of **1**. The EPR spectrum of **2** is characteristic of a high-spin Fe^{III} species in a nearly axial ligand field. We have determined all Mössbauer parameters for both complexes by a numerical treatment of applied field Mössbauer data. Species **1** exhibits an isomer shift $\delta_{/Fe}$ = 0.16 mm/s and a quadrupole splitting ΔE_Q = −2.08 mm/s (T = 4.2 K). In the case of **2**, we obtain an isomer shift $\delta_{/Fe}$ = 0.63 mm/s and a quadrupole splitting ΔE_Q = 1.12 mm/s (T = 4.2 K). These values are close to those published very recently by Bill et al. for [Fe(trispicMeen)(OOH)]$^{2+}$ (**3**) and [Fe(trispicMeen)(η^2–OO)]$^{+}$ (**4**) species, where bztpen and trispicMeen ligands differ by a noncoordinating group [A. J. Simaan, F. Banse, J.-J. Girerd, K. Wieghardt, E. Bill, *Inorg. Chem.* **2001**, *40*, 6538–6540]. We have also used the extension of the Griffith model developed by Lang et al. for Mössbauer spectroscopy [W. T. Oosterhuis, G. Lang, *Phys. Rev.* **1969**, *178*, 439–456] to evaluate the ^{57}Fe hyperfine tensor of **1** and reproduce the experimental data. On comparison with the Mössbauer data available for η^2-peroxo Fe^{III} complexes, our Mössbauer study of **2** agrees well with a high-spin Fe^{III} side-on peroxo complex. Very characteristic $\delta_{/Fe}$ and ΔE_Q ranges for hydrogenperoxo and side-on peroxo Fe^{III} species are now available, which should aid in the detection of comparable species formed in biological systems.

Introduction

There is currently great interest in non-heme peroxo species, since they are suspected to be key intermediates in several enzymatic or metabolic processes.[1] Detailed spectroscopic characterizations of peroxo species for diiron enzymes such as ribonucleotide reductase and methane monooxygenase are available in the literature.[1b] Where non-heme mononuclear peroxo intermediates are concerned, a well known example is the antitumor drug bleomycin: when this protein is exposed to dioxygen, a transient activated form involved in DNA-cleaving activity is formed. This has been demonstrated to be a hydrogenperoxo FeOOH species.[2] Peroxo species have also been proposed for mononuclear, non-heme, Fe-based superoxide dismutase[3] and more recently, from pulsed radiolysis studies, for the product of superoxide reductase reaction with superoxide.[4] In the recent past, several non-heme mononuclear peroxo model complexes, generated in solution, have been described in the literature.[5] Raman spectroscopy has been fruitful for gaining insight into the peroxo ligand binding mode; hydrogenperoxo and side-on (η^2) peroxo coordination geometries have been characterized.[5i] These two species have very different reactivities. Hydrogenperoxo species

[a] Laboratoire de Physicochimie des Métaux en Biologie, FRE CEA/CNRS/UJF 2427, Département de Réponse et Dynamique Cellulaires CEA/Grenoble,
38054 Grenoble Cedex 9, France
Fax: (internat.) +33−(0)438785090
E-mail: horner@cea.fr
[b] Service de Physique de l'Etat Condensé, Département de Recherche sur l'Etat Condensé, les Atomes et les Molécules, CEA/Saclay,
91191 Gif-sur-Yvette Cedex, France
[c] Department of Chemistry, University of Southern Denmark, Odense Campus,
5230 Odense M, Denmark
Supporting information for this article is available on the WWW under http://www.eurjic.org or from the author.

are believed to intervene in oxidation and hydroxylation reactions of substrates, and are likely to operate by the cleavage of the activated O−O bond to generate a catalytically active high-valent iron intermediate. In contrast, the O−O bond in a side-on peroxo complex is not activated for direct cleavage and the species is relatively stable, but can react as a nucleophile towards protonation, probably to produce highly reactive species.[6] No η^2-FeO_2 peroxo species has yet been characterized by Mössbauer spectroscopy in biological systems. A well known example of an η^2-FeO_2 peroxo model complex is $[Fe(edta)(O_2)]^{3-}$, which has been studied by many spectroscopic techniques,[6] including a recently detailed Mössbauer spectroscopy study.[7]

Indeed, Mössbauer spectroscopy is particularly well adapted for the study of iron compounds.[8] Nevertheless, few Mössbauer data for non-heme peroxide species are currently available in the literature.[7,9] We therefore decided to study the hydrogenperoxo complex $[^{57}Fe(bztpen)(OOH)]^{2+}$ (**1**) and its deprotonation product $[^{57}Fe(bztpen)(O_2)]^{2+}$ (**2**) [bztpen stands for *N*-benzyl-*N*,*N*′,*N*′-tris(2-pyridylmethyl)-ethane-1,2-diamine[10]] by Mössbauer spectroscopy. The two complexes **1** and **2** can be interchanged by a protonation-deprotonation sequence as shown in Scheme 1.

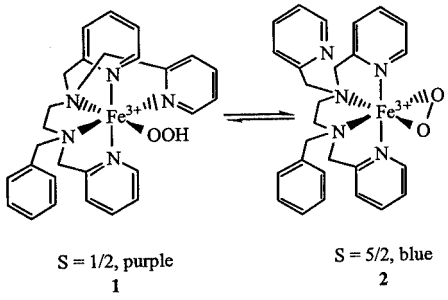

Scheme 1

While this work was nearing completion, Bill et al. published a detailed Mössbauer study of non-heme Fe^{III} hydrogenperoxo $[Fe(trispicMeen)(OOH)]^{2+}$ (**3**) and η^2-peroxo $[Fe(trispicMeen)(O_2)]^{+}$ (**4**) complexes [trispicMeen stands for *N*-methyl-*N*,*N*′,*N*′-tris(2-pyridylmethyl)ethane-1,2-diamine].[9b]

In this article we report the complete Mössbauer spectroscopy study of complexes **1** and **2**. The characteristic Mössbauer parameters obtained for each compound are in full agreement with Bill's results[9b] and give clear Mössbauer signatures for both non-heme mononuclear hydrogenperoxo and side-on peroxo species. This should aid in the detection of comparable species formed in biological systems.

Results

The ligand bztpen was prepared as described previously.[10] For the synthesis of $[^{57}Fe(bztpen)Cl](ClO_4)_2$, $^{57}FeCl_3{\cdot}6H_2O$ was used as a starting compound. Addition of $NaClO_4{\cdot}H_2O$ resulted in the immediate precipitation of the complex $[^{57}Fe(bztpen)Cl](ClO_4)_2$. The purple hydrogenperoxo complex **1** was generated in solution by treatment of $[^{57}Fe(bztpen)Cl]^{2+}$ with a large excess of hydrogen peroxide. Addition of 30 equivalents of triethylamine to this solution gave **2**, in which it has been proposed that the peroxo ligand is coordinated in the η^2 mode.[10] Both species were studied in detail by EPR and Mössbauer spectroscopy as described below.

EPR Spectroscopy

The hydrogenperoxo species **1** was studied by X-band EPR spectroscopy at low temperature. Figure 1 shows the EPR spectrum of **1** in methanol at $T = 6.3$ K; it is typical of a $S = 1/2$ low-spin Fe^{III} species, with g values observed at $g_{max} = 2.22$, $g_{inter} = 2.18$ and $g_{min} = 1.97$.

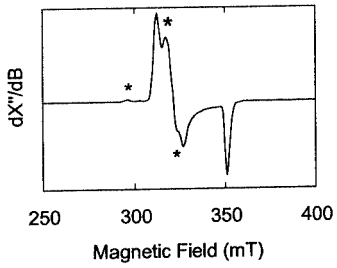

Figure 1. X-band EPR spectrum of **1** in methanol. EPR conditions : temperature 6.3 K, microwave frequency 9.678 GHz, power 2 mW, modulation 1.0 mT/100 kHz. The asterisks denote the components of a minor amount of $[^{57}Fe^{III}(bztpen)(OCH_3)]^{2+}$.

The stars in Figure 1 denote the components of the EPR signal arising from a minor amount (less than 1%) of a precursor species, which corresponds to the low-spin $[Fe^{III}(bztpen)(OCH_3)]^{2+}$.[10]

The 4.2 K X-band EPR spectrum of **2**, shown in Figure 2, exhibits signals at $g = 7.6$ and $g = 5.8$ and a broad unresolved signal in the $g = 4.5$ region.

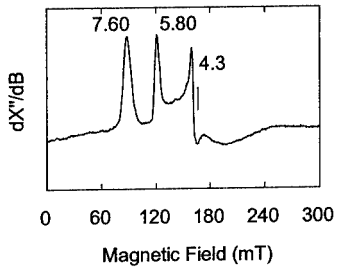

Figure 2. X-band EPR spectrum of **2** in methanol. EPR conditions: temperature 6.3 K, microwave frequency 9.678 GHz, power 20 mW, modulation 1.0 mT/100 kHz.

In addition, an EPR signal arising from a high-spin Fe^{III} contaminant in a rhombic ligand field is seen at $g = 4.3$, but the EPR signal of **1** has completely disappeared, indicating its quantitative transformation upon addition of triethylamine (data not shown). The spectrum of **2** is characteristic of a $S = 5/2$ Fe^{III} complex in a nearly axial ligand field and was analyzed by the rhombogram method.[11] For an $S = 5/2$ spin multiplet, observation of resonances at $g =$

Table 1. Mössbauer parameters for **1** and **2** at $T = 4.2$ K; published spin Hamiltonian parameters for non-heme Fe^{III} peroxo complexes with nitrogen ligands are also given for purposes of comparison; for **1**, with $g_x = -2.18$, $g_y = 2.22$ and $g_z = -1.97$, $A_x = 4.30$ T, $A_y = 6.26$ T and $A_z = 42.26$ T are obtained in the fitting procedure (n.a.: not available)

Compound	**1**	**3**	$[Fe(N_4P_y)(OOH)]^{2+}$	**2**	**4**	$[Fe(N_4P_y)(O_2)]^{+}$	$[Fe(edta)(O_2)]^{3-}$
Spin	1/2	1/2	1/2	5/2	5/2	5/2	5/2
D (cm^{-1})				−0.90	−1.7	n.a.	−1.0
E/D				0.08	0.08	n.a.	0.21
g_x	2.18	2.12	2.16	2.0	2.0	2.0	2.0
g_y	2.22	2.19	2.11	2.0	2.0	2.0	2.0
g_z	1.97	1.95	1.98	2.0	2.0	2.0	2.0
$A_x/g_n\beta_n$ (T)	−4.31	7.77	−6.63	−20.3	−22.71	−21.5	−23.1
$A_y/g_n\beta_n$ (T)	6.62	−3.65	4.45	−22.4	−22.09	−21.6	−21.4
$A_z/g_n\beta_n$ (T)	−42.26	−41.09	−38.42	−20.3	−20.40	−20.3	−20.8
ΔE_Q (mm/s)	−2.07	−2.01	1.62	+1.12	+1.37	n.a.	+0.72
η	0.26	0.4	n.a.	0.0	0.98	n.a.	0.4
$\delta_{/Fe}$ (mm/s)	+0.17	+0.19	+0.17	+0.63	+0.64	+0.61	+0.65
Euler angles	α = 64°	α = 43°	n.a.			n.a.	
reference	this work	[9b]	[9a]	this work	[9b]	[9a]	[7]

7.6, 5.8 and 4.5 is consistent with E/D ≈ 0.08. In particular, the signal at $g = 7.6$ arises from the $M_s = \pm 1/2$ Kramers doublet and the signal at $g = 5.8$ arises from the $M_s = \pm 3/2$ Kramers doublet. The temperature dependence of these signals is consistent with the $M_s = \pm 1/2$ doublet being the highest in energy (Supporting Information; see also footnote on the first page of this article). Consequently, the zero-field splitting parameter D must be negative for **2**, as for $[Fe(edta)O_2]^{3-}$ and **4** (Table 1).

Mössbauer Spectroscopy

The hydrogenperoxo complex **1** was studied by Mössbauer spectroscopy at low temperature in one low and two high magnetic fields applied parallel to the propagation direction of the Mössbauer γ-rays. Figure 3 shows Mössbauer spectra of **1** at $T = 4.2$ K ($H = 50$ mT, $H = 3$T) and $T = 10$ K ($H = 7$ T).

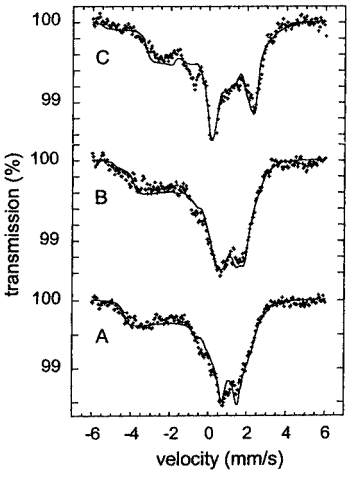

Figure 3. Mössbauer spectra in **1** in methanol. The experimental spectra taken at $T = 4.2$ K in an applied parallel field of 50 mT (A) and 3 T (B) and at $T = 10$ K in an applied parallel field of 7.0 T (C), were fitted (solid curves) with the parameters set of Table 1.

The rather featureless spectra obtained can be fitted simultaneously in the slow relaxation limit within the spin Hamiltonian formalism using a unique set of parameters. We were not fully able to reproduce the shape of the feature at velocity of about −1 mm/s in the 7 T spectrum (Figure 3, curve C). No high-spin Fe^{III} impurity was detected on a higher velocity scale (data not shown). The minor amount of precursor species $[Fe^{III}(bztpen)(OCH_3)]^{2+}$ discernible in the EPR spectrum of **1** was not taken into account in the Mössbauer fitting data. The g-values were taken as positive and fixed to the values obtained by EPR spectroscopy, with $g_x = 2.18$, $g_y = 2.22$ and $g_z = 1.97$ (vide infra). This is not a restriction, as a Mössbauer spectrum is only sensitive to the sign of the products $A_i \cdot g_i$, $i = x, y, z$[12] The Mössbauer parameters obtained from the fit are listed in Table 1.

At $T = 4.2$ K, complex **1** exhibits an isomer shift $\delta_{/Fe} = 0.17$ mm/s. This parameter, which is typical for a low-spin Fe^{III} complex, is similar to those published for hydrogenperoxo complexes with nitrogen ligands (Table 1). The quadrupole splitting $\Delta E_Q = -2.07$ mm/s is large and negative, and the asymmetry parameter $\eta = 0.26$ is low. Our fit was improved by introducing an Euler angle $\alpha = 64°$ between the [A] and [V] tensors. This means that the [A], [g] and [V] tensors share the same principal z axis. These experimentally ascertained values are close to those obtained for **3**[9b] and for the hydroperoxo complex $[Fe(N_4Py)(OOH)]^{2+}$, where N_4Py stands for *N*-[bis(2-pyridyl)methyl]-*N*,*N*-bis(2-pyridylmethyl)amine.[9a]

Complex **2** was studied by Mössbauer spectroscopy at low temperature in one small and one high magnetic field applied parallel to the propagation direction of the Mössbauer γ-rays. Figure 4 shows the Mössbauer spectra obtained at $H = 50$ mT ($T = 4.2$ K and 10 K) and at $H = 7$ T ($T = 4.2$ K).

These spectra were simultaneously fitted at the slow relaxation limit within the spin Hamiltonian formalism using a unique set of parameters. The Mössbauer parameters ob-

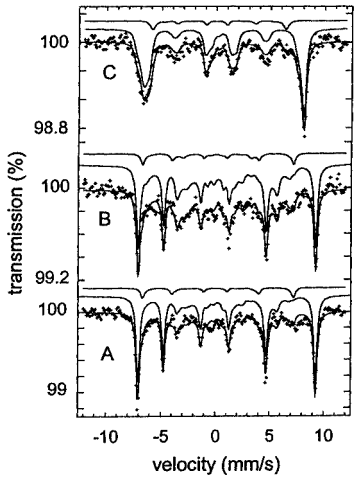

Figure 4. Mössbauer spectra in **2** in methanol. The experimental spectra taken at $T = 4.2$ K (A) and $T = 10$ K (B) in an applied parallel field of 50 mT, and at $T = 4.2$ K in an applied parallel field of 7.0 T (C), were fitted (solid curves) with the parameters set of Table 1. A Fe^{III} impurity (9.4 %) is also present. The solid curves located above the experimental spectrum show the contribution of both species (dashed lines).

tained from the fit are given in Table 1. The spectra of **2** are superimposed by the sextuplet spectra of a minor (9.4%) high-spin Fe^{III} component ($D = +2.9$ cm^{-1}, $E/D = 0.33$, $g = 2.0$, $[A]/g_n\beta_n = -18.0$ T), probably a degradation product of the peroxo complex.

At $T = 4.2$ K under a small applied field ($H = 50$ mT), complex **2** exhibits a sextuplet Mössbauer spectrum. The internal field can be evaluated from its overall splitting and is about 54 T. This is typical for a high-spin Fe^{III} complex. The axial zero-field parameter D is found to be of the order of -1 cm^{-1}, and is close to the D values already published for $[Fe(edta)(O_2)]^{3-}$ and for **4** (Table 1). For $E/D = 0.08$ (zero-field splitting parameter $D < 0$), the lower Kramers doublet $M_s = \pm 5/2$ is uniaxial (it has an easy axis of magnetization along z) and yields a sextuplet Mössbauer spectrum.[13] At $T = 4.2$ K, the levels of population of the upper doublets are much smaller than that of the ground doublet. Therefore, the observed Mössbauer spectrum at $T = 4.2$ K is attributed to the $M_s = \pm 5/2$ doublet and measures the V_{zz} component of the electric field gradient tensor [V]. It can be seen from the experimental spectrum that V_{zz} is positive, as the inner transitions are shifted to the left of the spectrum, and so ΔE_Q is positive for **2**.[13] A Mössbauer spectrum of **2** recorded at higher temperature should give an insight into the other components of the electric field gradient V_{xx} and V_{yy} and allow the asymmetry parameter $\eta = (V_{xx} - V_{yy})/V_{zz}$ to be determined.[7,13] The spectrum recorded at $T = 10$ K and $H = 50$ mT is shown in Figure 4, part B: several additional features appear as the contributions of the middle and upper Kramers doublets (which are not uniaxial) increase. By simultaneous fitting of the three experimental spectra, a value of $\eta = 0$ and a large positive quadrupole splitting $\Delta E_Q = +1.12$ mm/s were determined for **2**. A large isomer shift value $\delta_{/Fe} = 0.63$ mm/s is obtained for this high-spin Fe^{III} complex. The hyperfine coupling tensor of **2** is negative ($A_{av}/g_n\beta_n = -21$ T) because of the main contribution of the Fermi contact term and slightly anisotropic, as for $[Fe(edta)(O_2)]^{3-}$, **4** and the η^2-peroxo complex $[Fe(N_4Py)(O_2)]^+$ (Table 1).

Discussion

The theoretical model developed by Griffith[14] and adapted by Taylor[15] is commonly used to evaluate the tetragonal and rhombic field parameters Δ/λ and V/λ, respectively (where λ is the spin-orbit coupling constant), of low-spin ferric complexes from their g-values determined by EPR spectroscopy. Such a calculation assumes a symmetry not lower than rhombic, a condition not always met, as discussed below for **1**. Therefore, in this model the electronic [g] tensor, the magnetic hyperfine [A] tensor and the electric field gradient [V] tensor are assumed to have a common axis system.[12] Moreover, the orbital reduction factor k is taken to be equal to 1.[14] Following the proposal of Girerd et al. for **3**, the product $g_x.g_y.g_z$ is taken to be positive (with $g_x = -2.18$, $g_y = 2.22$, $g_z = -1.97$),[5] as initially shown by Burger et al.[16] We selected the system of axes described by Taylor, such that $|V| < (2/3)|\Delta|$, where the three real coefficients a, b and c of the ground Kramers doublet are given by the following Equations:[15]

$$\begin{aligned} a &= (g_z + g_y)[8(g_z + g_y - g_x)]^{-1/2} \\ b &= (g_z - g_y)[(g_z + g_y - g_x)]^{-1/2} \\ c &= (g_y - g_x)[(g_z + g_y - g_x)]^{-1/2} \end{aligned} \quad (1)$$

From the experimental g values, we obtain: $a = 0.0567$, $b = 0.0476$ and $c = 0.9979$, which in turn give the field parameters $\Delta/\lambda = -10.10$ and $V/\lambda = 1.85$.[5g,5i,15] This set of values implies that the unpaired electron is located in an orbital with a predominant d_{xy} character, which is strongly destabilized by an antibonding interaction with the π^* orbital of the OOH ligand.[5g,5i] The field parameters of **1** are close to those obtained by Girerd et al. for the hydrogenperoxo complex **3** involving a nitrogen ligand with a similar coordinating environment.[5g,5i] These results agree with a $(d_{xz})^2(d_{yz})^2(d_{xy})^1$ low-spin Fe^{III} electronic configuration, which gives a large negative V_{zz} value (and a large negative ΔE_Q) and a small asymmetry parameter, as found experimentally (Table 1).

By use of the extension of the Griffith model developed by Lang et al. for Mössbauer spectroscopy, one can evaluate the ^{57}Fe hyperfine tensor; the hyperfine tensor values are given by:[17]

$$A_x = -P[-4bc - (1 + \kappa)(a^2 - b^2 - c^2) + 3/7(a^2 - 3b^2 - 3c^2 + 2ab + 2ac)]$$

$$A_y = -P[4ac - (1 + \kappa)(a^2 - b^2 + c^2) + 3/7(3a^2 - b^2 + 3c^2 - 2ab - 2bc)]$$

$$A_z = -P[4ab - (1 + \kappa)(a^2 + b^2 - c^2) + 3/7(3a^2 + 3b^2 - c^2 - 2ac - 2bc)]$$

where a, b and c are given by Equation (1), κ is a parameter characterizing the isotropic contact contribution ($\kappa =$

0.35 for low-spin ferric heme proteins) and P is a scaling factor accounting for the radial distribution of the valence electrons of the Fe^{III} ion ($P/g_n\beta_n \approx -62$ T for low-spin ferric heme proteins).[18] It was possible to reproduce the anisotropic experimental [A] tensor by choosing $\kappa = 0.35$ and $P/g_n\beta_n = -50.3$ T.

[A]/$g_n\beta_n$ (−3.92; 6.09; 42.15) was obtained ($A_{iso}/g_n\beta_n$ = 14.8 T). The low value obtained for P indicates higher covalency for the low-spin iron ion in **1** than for low-spin ferric ions in heme proteins and activated bleomycin.[16]

It is worth noting that different approaches are used in the literature to deal with the signs of the g-values to be employed within the Griffith model. In the case of "activated bleomycin" $Fe^{III}OOH$, Solomon et al. concluded that the three g-values should be taken to be positive.[19] Indeed, they argued that other signs of the g-values would produce crystal field parameters V and Δ that would not allow the experimentally determined higher-energy intra-t_{2g} transition to be reproduced ($E_{exp} \approx 3800$ cm^{-1}). They used an axis system in which the z-axis (which corresponds to the y-axis in this paper) was taken along the Fe−hydrogenperoxo bond. On the other hand, different signs ($g_x = -2.17$; $g_y = 2.26$; $g_z = -1.94$) were obtained by Girerd et al.[5i] for "activated bleomycin" under the same assumption as made by Scholes et al.[20] that $g_xg_yg_z$ is positive. Moreover, upon using the crystal field parameters determined from the latter g-values, one obtains a higher-energy intra-t_{2g} transition at 3900 cm^{-1} (using a covalently reduced spin-orbit coupling constant[19] of 380 cm^{-1} for Fe^{III}). This value is very close to that of 3950 cm^{-1} predicted from field parameters with g_x, g_y and g_z taken to be all positive,[19] and not in contradiction with the near IR MCD results. To probe this point further, we carried out simultaneous fitting of the Mössbauer data for **1** with g_x, g_y and g_z all positive, z being along the Fe−hydrogenperoxo bond. Identical fits were obtained, but with Mössbauer parameters expressed in the new coordinate system.

As noted by Münck et al.[18b] and reemphasized in the case of **3** by Bill et al.,[9b] the Griffith-Taylor model might not be fully valid when the symmetry is less than rhombic. It can be seen in the EPR spectrum of **1** (Figure 1) that the $g_z = 1.97$ resonance does not exhibit any ^{57}Fe magnetic hyperfine splitting. On the other hand, a large component of the hyperfine coupling tensor along the z-axis of the [A] proper axis system is determined experimentally. These conflicting observations can be reconciled if the principal axis frames of the [A] and [g] tensors of **1** are rotated relative to each other. Such a case has already been observed for the low-spin Fe^{III} centre in the active nitrile hydratase.[18b]

Finally, it must be noted that the isomer shift and the quadrupole splitting of **1** are within the range observed for hydrogenperoxo Fe^{III} complexes ($\delta_{/Fe} = 0.16-0.19$ mm/s and a large and negative $\Delta E_Q \approx -2.0$ mm/s at $T = 4.2$ K). These parameters match those of activated bleomycin ($\delta_{/Fe} = 0.16$ mm/s and $\Delta E_Q = -2.96$ mm/s at T = 4.2 K),[16] substantiating the proposition that **1** is a relevant model for these biological hydroperoxo non-heme iron species.

The isomer shift value $\delta_{/Fe} = 0.63$ mm/s obtained for **2** is large for a high-spin Fe^{III} complex but is located in the 0.61−0.65 mm/s range that characterizes high-spin Fe^{III}-η^2O_2 complexes, as shown in Table 1. The side-on peroxo complexes in Table 1 are also characterized by positive ΔE_Q values in the 0.72−1.37 mm/s range ($T = 4.2$ K). Isomer shifts above 0.60 mm/s up to 0.68 mm/s have also been reported in the literature for dinuclear Fe^{III} peroxo complexes, which generally exhibit ΔE_Q values greater than 1.50 mm/s, although some exceptions exist.[22] An isomer shift $\delta_{/Fe}$ = 0.67 mm/s ($T = 4.2$ K) has also been reported for the high-spin porphyrin Fe^{III} η^2-O_2 complex $[Fe(OEP)(O_2)]^-$ (OEP stands for the octaethylporphyrin dianion ligand).[23] In addition, a large quadrupole splitting is observed for **2**, as for the series of side-on peroxo complexes in Table 1. This specific feature is probably due to the 3d anisotropy introduced by the η^2-FeO_2 binding mode, as suggested by theoretical calculations.[24]

Conclusion

The Mössbauer parameters obtained for **1** and **2** in this study agree with the proposal of McKenzie et al. that **1** is a hydrogenperoxo complex and **2** an η^2-peroxo Fe^{III} complex.[10] The coordination number of Fe^{III} in **2** (7 or 6) still remains unknown, the latter being obtained with the decoordination of a picolyl arm of bztpen; the isolation and crystallization of such a species would be useful.

Table 1 shows that non-heme hydrogenperoxo and side-on peroxo Fe^{III} complexes exhibit very characteristic and unambiguous isomer shift values, and $\delta_{/Fe}$ and ΔE_Q ranges are now available for both types of mononuclear peroxo complexes. In particular, no confusion is possible between a mononuclear Fe^{III} species of biological interest with nitrogen/oxygen or sulfur ligands and a mononuclear Fe^{III}-η_2O_2 species. This should make the Mössbauer identification of such species possible in biological systems.

In addition, the Mössbauer parameters obtained here reemphasize both the peculiarity of peroxo Fe^{III} derivatives among ferric complexes and their similarity with their nitrosyl analogues. Indeed, η_2-O_2 iron complexes and $[FeNO]^7$ ($S = 3/2$) species display high isomer shifts, and theoretical descriptions show in both cases that the metal-ligand bond involves a strong σ bonding and a weak additional Π interaction.[24,25]

Experimental Section

EPR spectra were recorded on a Bruker EMX spectrometer. For low-temperature studies, an Oxford Instruments continuous-flow helium cryostat and a temperature control system were used.

All Mössbauer measurements were performed with a constant acceleration spectrometer calibrated with hematite, and isomer shifts are reported relative to an Fe metal standard at room temperature. Variable-temperature experiments were carried out with the sample placed in the tail section of a variable-temperature cryostat. The

temperature of the sample was regulated to within 0.2 K with a conventional PID system. The samples for Mössbauer spectroscopy contained ≈ 4 mM ^{57}Fe in a 200 μL nylon cell. The Mössbauer spectra were analysed with the WMOSS (WEB Research, Edina, MN) software package. For the analysis, the Hamiltonian **H** describing the system is used:

$$\mathbf{H} = D[\mathbf{S}_z^2 - (1/3)S(S+1) + (E/D)(\mathbf{S}_x^2 - \mathbf{S}_y^2)] + \beta_e \cdot \mathbf{S} \cdot [g] \cdot \mathbf{B} + \langle \mathbf{S} \rangle \cdot [A] \cdot \mathbf{I} - g_n \beta_n \mathbf{B} \cdot \mathbf{I} + \mathbf{H_Q}$$

where D and E are the axial and rhombic zero field splitting parameters, respectively, β_e the electronic Bohr magneton, [g] the electronic g-tensor, $\langle \mathbf{S} \rangle$ the appropriately taken spin expectation value, [A] the magnetic hyperfine tensor, g_n the nuclear g-factor, β_n the nuclear Bohr magneton and $\mathbf{H_Q}$ the quadrupolar interaction Hamiltonian.

Synthesis of [^{57}Fe(bztpen)Cl](ClO$_4$)$_2$ and of Complexes 1 and 2

Caution: Although no problems were encountered in the preparation of the perchlorate salts, care should be taken when handling such potentially hazardous compounds.

The ligand bztpen was synthesized as previously described.[10] The $^{57}FeCl_3 \cdot 6H_2O$ starting compound was obtained as recently published.[7] Methanol was purchased from Prolabo, $NaClO_4$ from Sigma, hydrogen peroxide and triethylamine from Aldrich, and all were used without further purification. For the synthesis of [^{57}Fe(bztpen)Cl](ClO$_4$)$_2$, $^{57}FeCl_3 \cdot 6H_2O$ (53.2 mg, 0.197 mmol) in dry methanol (1 mL) was added to a solution of bztpen (83.3 mg, 0.197 mmol) in 2 mL of dry methanol. A yellow precipitate formed immediately and redissolved spontaneously after 2 minutes. Addition of $NaClO_4$ (72.6 mg, 0.591 mmol) resulted in precipitation of a yellow product, which was isolated by filtration. Treatment of this yellow compound, dissolved in dry methanol, with hydrogen peroxide (30%, 300 equivalents) generated the purple species **1**. Addition of triethylamine (99%, 30 equivalents) produced a blue solution of **2**.

Acknowledgments

N. Genand-Riondet (CEA/Saclay) is thanked for recording Mössbauer experiments and helping in the design of Mössbauer cells for the in-field experiments.

[1] [1a] L. Que, R. Y. Ho, *Chem. Rev.* **1996**, *96*, 2607−2624. [1b] E. I. Solomon, T. C. Brunold, M. I. Davis, J. N. Kemsley, S.-K. Lee, N. Lehnert, F. Neese, A. J. Skulan, Y.-S. Yang, J. Zhou, *Chem. Rev.* **2000**, *100*, 235−349. [1c] M. Costas, K. Chen, L. Que, Jr., *Coord. Chem. Rev.* **2000**, 200−202, 517−544.

[2] [2a] J. W. Sam, X.-J. Tang, J. Peisach, *J. Am. Chem. Soc.* **1994**, *116*, 5250−5256. [2b] R. J. Guajardo, J. D. Tan, P. K. Mascharak, *Inorg. Chem.* **1994**, *33*, 2838−2840.

[3] [3a] C. Bull, J. A. Fee, *J. Am. Chem. Soc.* **1985**, *107*, 3295−3304. [3b] D. M. Dooley, J. L. Karas, T. F. Jones, C. E. Coté, S. B. Smith, *Inorg. Chem.* **1986**, *25*, 4761−4766.

[4] [4a] M. Lombard, C. Houée-Levin, D. Touati, M. Fontecave, V. Nivière, *Biochemistry* **2001**, *16*, 5032−5040. [4b] M. D. Clay, F. E. Jenney, Jr., P. L. Hagedoorn, G. N. George, M. W. W. Adams, M. K. Johnson, *J. Am. Chem. Soc.* **2002**, *124*, 788−805.

[5] [5a] I. Bernal, I. M. Jensen, K. B. Jensen, C. J. McKenzie, H. Toftlund, J. P. Tuchagues, *J. Chem. Soc., Dalton Trans.* **1995**, 3667−3675. [5b] C. Kim, K. Chen, J. Kim, L. Que, Jr., *J. Am. Chem. Soc.* **1997**, *119*, 5964−5965. [5c] M. Lubben, A. Meetsma, E. C. Wilkinson, B. Feringa, L. Que, Jr., *Angew. Chem. Int. Ed. Engl.* **1995**, *34*, 2048− 2051. [5d] Y. Zhang, T. E. Elgren, Y. Dong, L. Que, Jr., *J. Am. Chem. Soc.* **1993**, *115*, 811−813. [5e] K. B. Jensen, C. J. McKenzie, L. P. Nielsen, J. Z. Pedersen, H. M. Svendsen, *Chem. Commun.* **1999**, 1313−1314. [5f] A. J. Simaan, F. Banse, P. Mialane, A. Boussac, S. Un, T. Kargar-Grisel, G. Bouchoux, J.-J. Girerd, *Eur. J. Inorg. Chem.* **1999**, 993−996. [5g] A. J. Simaan, S. Döpner, F. Banse, S. Bourcier, G. Bouchoux, A. Boussac, P. Hildebrandt, J.-J. Girerd, *Eur. J. Inorg. Chem.* **2000**, 1627−1633. [5h] A. Hazell, C. J. McKenzie, L. P. Nielsen, S. Schindler, M. Weitzer, *J. Chem. Soc., Dalton Trans.* **2002**, 310−317. [5i] J.-J. Girerd, F. Banse, A. J. Simaan, *Struture and Bonding*, Springer-Verlag, New York, **2000**, 97, 145−177.

[6] F. Neese, E. I. Solomon, *J. Am. Chem. Soc.* **1998**, *120*, 12829−12848.

[7] O. Horner, C. Jeandey, J.-L. Oddou, P. Bonville, J.-M. Latour, *Eur. J. Inorg. Chem.* **2002**, 1186−1189.

[8] [8a] P. Gütlich, R. Link, A. Trautwein, Mössbauer Spectroscopy and Transition Metal Chemistry, Springer-Verlag, Berlin, **1979**. [8b] V. Schünemann, H. Winkler, *Rep. Prog. Phys.* **2000**, *63*, 263−353.

[9] [9a] V. Vrajmasu, E. Münck, R. Ho, L. Que, Jr., G. Roefles, B. L. Feringa, *J. Inorg. Biochem.* **2001**, *86*, 472. [9b] A. J. Simaan, F. Banse, J.-J. Girerd, K. Wieghardt, E. Bill, *Inorg. Chem.* **2001**, *40*, 6538−6540.

[10] A. Hazell, C. J. McKenzie, L. P. Nielsen, S. Schindler, M. Weitzer, *J. Chem. Soc., Dalton Trans.* **2002**, 310−317.

[11] H. H. Wickman, P. M. Klein, D. A. Shirley, *Phys. Rev.* **1966**, *152*, 345−357.

[12] B. H. Huynh, M. H. Emptage, E. Münck, *Biochim. Biophy. Acta* **1978**, *534*, 295−306.

[13] E. Münck in *Physical Methods in Bioinorganic Chemistry − Spectroscopy and Magnetism* (Ed.: L. Que, Jr.), University Science Books, **2000**, chapter 6.

[14] J. S. Griffith, *Proc. R. Soc. London, A* **1956**, *234*, 23−36.

[15] C. P. S. Taylor, *Biochim. Biophys. Acta* **1977**, *491*, 137−149.

[16] R. M. Burger, T. A. Kent, S. B. Horwitz, E. Munck, J. Peisach, *J. Biol. Chem.* **1983**, *258*, 1559−1564.

[17] W. T. Oosterhuis, G. Lang, *Phys. Rev.* **1969**, *178*, 439−456.

[18] [18a] G. Lang, *Q. Rev. Biophys.* **1970**, *3*, 1−60. [18b] V.-C. Popescu, E. Münck, B. G. Fox, Y. Sannakis, J. G. Cummings, I. M. Turner, Jr., M. J. Nelson, *Biochemistry* **2001**, *40*, 7984−7991.

[19] F. Neese, J. M. Zaleski, K. L. Zaleski, E. I. Solomon, *J. Am. Chem. Soc.* **2000**, *122*, 11703−11724.

[20] A. Veselov, H. Sun, A. Sienkiewicz, H. Taylor, R. M. Burger, C. P. Sholes, *J. Am. Chem. Soc.* **1995**, *117*, 7508−7512.

[21] J. W. Sam, X.-Jun Tang, J. Peisach, *J. Am. Chem. Soc.* **1994**, *116*, 5250−5256.

[22] C. Hauser, T. Glaser, E. Bill, T. Weyermüller, K. Wieghardt, *J. Am. Chem. Soc.* **2000**, *122*, 4352−4365.

[23] J. A. Broadwater, C. Achim, E. Münck, B. G. Fox, *Biochemistry* **1999**, *38*, 12197−12204 and references therein.

[24] J. N. Burstyn, J. A. Roe, A. R. Miksztal, B. A. Shaevitz, G. Lang, J. S. Valentine, *J. Am. Chem. Soc.* **1988**, *110*, 1382−1388.

[25] F. Neese, E. I. Solomon, *J. Am. Chem. Soc.* **1998**, *120*, 12829−12848.

[26] C. A. Brown, M. A. Pavlosky, T. E. Westre, Y. Zhang, B. Hedman, K. O. Hodgson, E. I. Solomon, *J. Am. Chem. Soc.* **1995**, *117*, 715−732.

Received March 22, 2002
[I02154]